Selective COX-1 inhibition as a target of theranostic novel diarylisoxazoles

5 **AUTHORS**, INCLUDING:

maria grazia Perrone
Università degli Studi di Bari Aldo Moro
50 PUBLICATIONS **468** CITATIONS

SEE PROFILE

Antonio Lavecchia
University of Naples Federico II
118 PUBLICATIONS **2,415** CITATIONS

SEE PROFILE

Antonio Scilimati
Università degli Studi di Bari Aldo Moro
79 PUBLICATIONS **925** CITATIONS

SEE PROFILE

Original article

Selective COX-1 inhibition as a target of theranostic novel diarylisoxazoles

CrossMark

Paola Vitale [a,1], Maria Grazia Perrone [a,1], Paola Malerba [a], Antonio Lavecchia [b,**], Antonio Scilimati [a,*]

[a] Department of Pharmacy & Pharmaceutical Sciences, University of Bari "A. Moro", Via Orabona 4, 70125 Bari, Italy
[b] Department of Pharmacy, "Drug Discovery" Laboratory, University of Naples Federico II, Via D. Montesano 49, 80131 Naples, Italy

ABSTRACT

Cyclooxygenase(COX)-1 role in some diseases is increasingly studied. 3-(5-Chlorofuran-2-yl)-5-methyl-4-phenylisoxazole (P6), a highly selective cyclooxygenase-1 inhibitor, was used as a "lead" to design new isoxazoles (2a–m), differently selective towards COX-1. Those isoxazoles might be useful as novel theranostic agents and also to better clarify COX-1 role in the human physiology and diseases. 2a–m were prepared in fair to good yields developing suitable synthetic strategies. They were evaluated in vitro for their COX-inhibitory activity and selectivity. Structure–activity relationship studies of the novel set of diarylisoxazoles allowed to identify new key determinants for COX-1 selectivity, and to uncover compounds appropriate for a deep pharmacokinetic and pharmacodynamic investigation. 3-(5-Chlorofuran-2yl)-4-phenylisoxazol-5-amine (2f) was the most active compound of the series, its inhibitory activity was assessed in purified enzyme (COX-1 IC_{50} = 1.1 μM; COX-2 IC_{50} > 50 μM) and in the ovarian cancer cell line (OVCAR-3) expressing only COX-1 (IC_{50} = 0.58 μM). Furthermore, the high inhibitory potency of 2f was rationalized through docking simulations in terms of interactions with a crystallographic model of the COX-1 binding site. We found critical interactions between the inhibitor and constriction residues R120 and Y355 at the base of the active site, as well as with S530 at the top of the side pocket.

© 2014 Published by Elsevier Masson SAS.

1. Introduction

Cyclooxygenase (COX) is the target of nonsteroidal anti-inflammatory drugs (NSAIDs) [1]. Two COX isoforms (COX-1 and COX-2) are known as a product of different genes [2]. COX-1 is considered a "housekeeping gene" by virtue of constitutive low-levels of expression in most cell types. However, high levels of constitutive COX-1 expression have been detected in the stomach and platelets, where it catalyzes the arachidonic acid (AA) conversion into prostaglandins capable to protect the gastrointestinal tract and to modulate platelet function. COX-2, even if promotes the same AA bis–oxygenation reaction, is mainly involved in inflammation and pain. The use of coxibs in humans allowed to unravel the protective role of COX-2 in the cardiovascular system mostly through the generation of prostacyclin [3]. COX-1 role in humans is quite vague except for platelet activation and gastrointestinal protection. The

former was enlightened by the use of aspirin, which is a preferential platelet COX-1 inhibitor when given at low-doses [4], whereas the latter was demonstrated indirectly using coxibs which spare COX-1 [5,6]. The use of COX-1 knockout mice enlightened the potential pathogenic contribution of prostanoids synthesized via COX-1 to inflammatory arthritis [7], atherogenesis [8], intestinal polyposis [9], carcinogenesis [10], neuroinflammation [11] and gastrointestinal bleeding and ulceration [12]. In addition, although COX-2 is over-expressed in most of cancer types, in human ovarian cancer the major expressed isoform is COX-1 where it promotes angiogenic growth factor production [13], as well as it is responsible of pain processing and sensitization in spinal cord and gracile nucleus after surgery [14]. Recently, a marked involvement of COX-1 in the very early stages of neurodegenerative diseases, with a marked inflammatory component, has also been demonstrated [15,16].

Thus, the availability of highly specific COX-1 inhibitors which better mirror pharmacological treatment in humans will be of valuable help to prove the role of COX-1 in human health and diseases [12].

Together with the classical NSAIDs aspirin and indomethacin, few examples of selective COX-1 inhibitors (mofezolac, SC-560, FR122047, P6, ABEX-3TF) have been reported so far as potential new analgesic and antiproliferative agents (Fig. 1) [17–23].
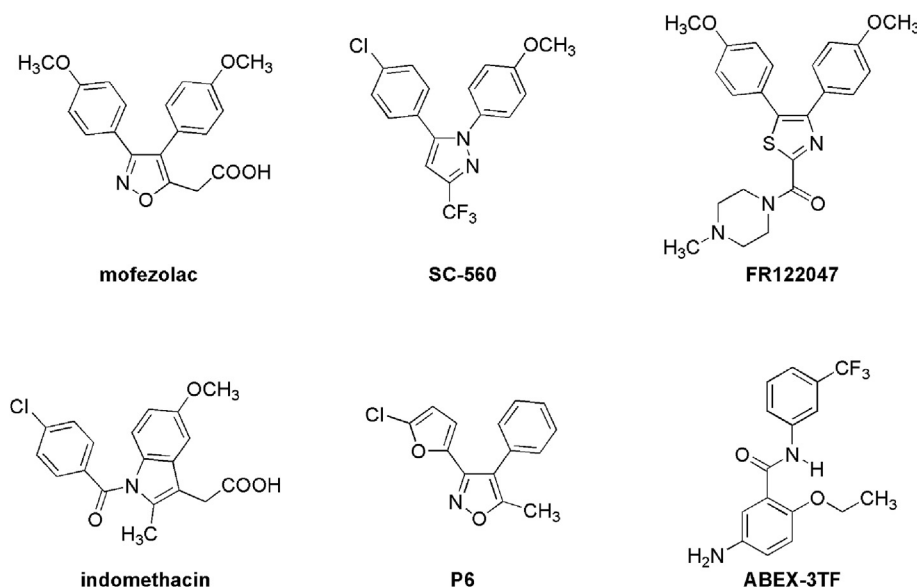

Fig. 1. Selective COX-1 inhibitors.

In one of our previous studies, we reported the 3-(5-chlorofuran-2-yl)-5-methyl-4-phenylisoxazole (**P6,** Fig. 1) as a highly selective COX-1 inhibitor [24,25], which allowed us to clarify and confirm that within the 3,4-diarylisoxazole class the *p*-sulfamoylphenyl group is essential for good COX-2 inhibitory potency, and the lack of the sulfonamide moiety reverse the COX-2 selectivity in favor of COX-1. Based on these findings, a novel set of selective COX-1 inhibitors has been synthesized, in order to recognize the molecular determinants necessary to have a selective diarylisoxazole COX-1 inhibitor, as well as to develop new compounds as new antiplatelet agents, analgesics, anti-inflammatories and chemopreventive drugs [26]. Moreover, structure–activity relationship studies of a series of diarylpyrazoles analogs of **P6** allowed us also to clarify that the isoxazole core ring and furyl group are crucial determinants for high COX-1 selectivity [27].

Herein, we report the synthesis of a set of novel **P6** analogs, designed collectively considering the known chemical and structural features to assure good COX-1 selectivity. New moieties are also explored (i.e., amino- and amido-group) aimed at developing both new pharmacological [26] and diagnostic tools [28]. The newly synthesized target compounds were evaluated for *in vitro* COX-1 and COX-2 inhibitory activity and selectivity. Furthermore, the affinity data of the most active inhibitors were rationalized through enzyme docking simulations in terms of interactions with a crystallographic model of the COX-1 binding site.

domain of PGHS. The crystal structure of ovine PGHS complexed with AA shows that, in the cyclooxygenase active site nineteen aminoacidic residues determine fifty contacts with the substrate: among them two are hydrophilic and forty-eight establish hydrophobic interactions [29].

This is the reason for which at least three different chemical classes of COXs inhibitors (carboxylic acids, diarylheterocycles, phenazones) exist. Coxibs development solved in part the selectivity problem in favor of COX-2. Their identification was triggered as an attempt to reduce or null the GI side effect associated to the poor COXs selectivity of most of *t*NSAIDs [12].

During the last two decades, as above-mentioned, few efforts were devoted to develop COX-1 inhibitors due to the scarce knowledge of its tissue/cell distribution and role in some human diseases onset and progression. On the contrary, a lot of work was performed to identify a large number of COX-2 inhibitors belonging to the chemical class of diarylheterocycles. The major difference between compounds of this class is the nature of the central ring. Thiazole, isoxazole, thiophene, cyclopentene structures and many others were proposed.

Recently, we studied the effect of the substitution of the heterocycle core ring on the COX-1 inhibition by maintaining some **P6** moieties and replacing the isoxazole central ring with pyrazole or thiazole [27].

2. Result and discussion

2.1. Design of new 3,4-diarylisoxazoles

Our discovery of **P6** [3-(5-chlorofuran-2-yl)-5-methyl-4-phenylisoxazole], a highly selective COX-1 inhibitor [24,25], prompted us to attempt more specific structural modifications without changing the isoxazole core ring, with the aim to investigate by SAR studies, how chemical moieties replacement could affect COX-1 selective inhibition.
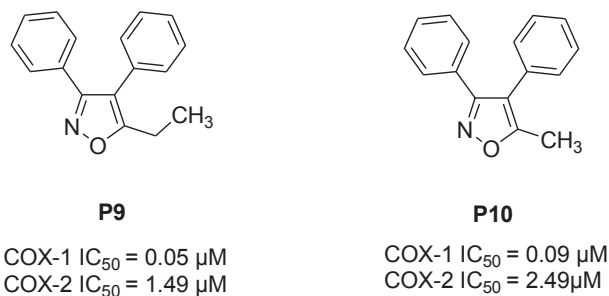
The selectivity towards COXs is still an open target. The cyclooxygenase active site is a long hydrophobic channel that protrudes from the membrane binding domain into the core of the globular

COX-1 IC$_{50}$ = 0.05 μM
COX-2 IC$_{50}$ = 1.49 μM

COX-1 IC$_{50}$ = 0.09 μM
COX-2 IC$_{50}$ = 2.49μM

Fig. 2. 3,4-Diphenyl-5-ethylisoxazole (**P9**) and 3,4-diphenyl-5-methyl-isoxazole (**P10**) analogs of **P6**.
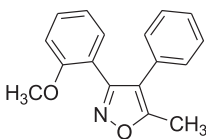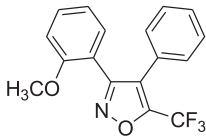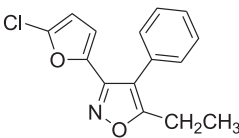
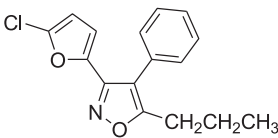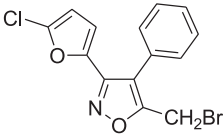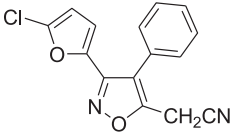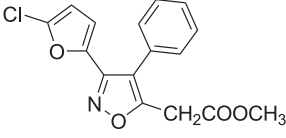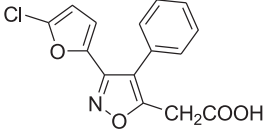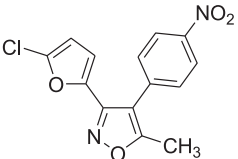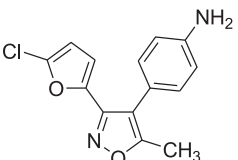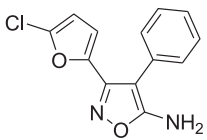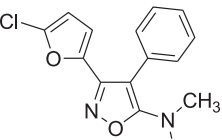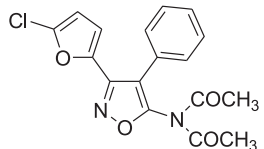Structural features of **P6** (Fig. 1) and its analogs 3,4-diphenyl-5-ethylisoxazole (**P9**, Fig. 2), 4-diphenyl-5-methyl-isoxazole (**P10**, Fig. 2) [24,25] were used to project new COX-1 inhibitors, taking into account that in the diarylheterocycles the size of the diaryls is one of the COX selectivity determinants (compare **P6**, **P9** and **P10** IC_{50} values; Fig. 2 and Table 3).

Diarylisoxazoles **2b**—**l** (Table 1) were designed to evaluate the effect of the C_5-substituent modification on the COX-1/COX-2 inhibitory activity, with the aim to identify, through a SAR study, further steric and electronic requirements for selective interactions at COX-1 active site. Furthermore, **2f**, **2g**, **2h** and **2l** were prepared to verify the importance of acidity or basicity of the substituent at C_5-isoxazole ring position for COX-inhibitory activity and -selectivity. **2e** and **2m** were prepared to study the influence of modification of the substituent on the phenyl at isoxazole-C_4 on COX-1 activity.

3-(5-Chlorofuran-2-yl)-4-phenylisoxazol-5-amine (**2f**) was found to be highly potent and selective COX-1 inhibitor. In contrast, its derivatives **2g** and **2h** did not inhibit COX activities. A similar result was observed when the substituent was a carboxylic group,

Table 1
Molecular recognition in the 3-(5-chlorofuran-2-yl)-5-methyl-4-phenylisoxazole (**P6**) analogs.

as for **2l**, designed as a **P6** derivative equivalent to mofezolac (Fig. 1). It was found scarcely active on COXs. To better rationalize such results, we investigate also the electronic effect of the substituent on the methylene at C_5, by evaluating *in vitro* COX-1 and COX-2 inhibitory activity and selectivity of isoxazoles **2c,d** and **2i**–**l**.

On the other hand, **2a** and **2b** were prepared to verify the role of the oxygen on the substituent on isoxazole-C_3, with the aim to identify a functional group alternative to the furan, to be usefully modified also in the preparation of radiolabelled compounds containing the $[^{11}C]$ as a radionuclide in the place of $[^{12}C]$ in CH_3O.

With the same objective we prepared the compound **2e**, designed as analog of **P6** with EWG on *para*-position of C_4 aromatic ring as well as intermediate in the preparation of radiolabelled compounds.

2.2. Chemistry

We prepared a number of 3,4-diarylisoxazoles **2a**–**e**, by a *one-pot* procedure, with fair to good yields, just reacting arylnitrile oxides with sodium enolates of 3-aryl-2-propanones **1a**–**e** (Scheme 1, Table 2) obtained by reacting the suitable propanone with NaH at 0 °C [25,30]. As previously found [24,25,31], we often observed the complete dehydration-aromatization of 5-hydroxyisoxazolines to the corresponding isoxazoles, and this occurs "spontaneously" in basic conditions, possibly by an E1cB mechanism [32], due to the presence of NaH in the reaction mixture.
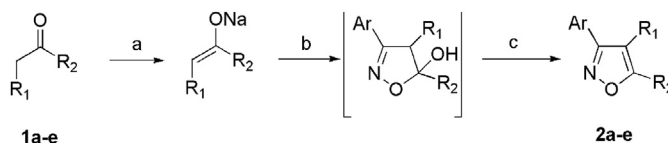
Scheme 1. Reagents and conditions: (a) NaH/THF, 1 h, 0 °C; (b) ArCNO/THF, 12 h, r.t.; (c) sat. aq. NH₄Cl.

Table 2
Yields of 3,4-diarylisoxazoles **2a**–**e** obtained by 1,3-dipolar cycloaddition of aryl-nitrile oxides to sodium enolates of 3-aryl-2-propanones **1a**–**e** and "*in situ*" subsequent dehydration/aromatization under basic conditions.

Ar	R_1	R_2	**2a**–**f** (yield (%))
2-Methoxyphenyl-	Phenyl	CH_3	**2a** (43)
2-Methoxyphenyl-	Phenyl	CF_3	**2b** (43)
5-Chlorofuran-2-yl-	Phenyl	CH_3	**P6** (60)
5-Chlorofuran-2-yl-	Phenyl	CH_2CH_3	**2c** (46)
5-Chlorofuran-2-yl-	Phenyl	$CH_2CH_2CH_3$	**2d** (21)
5-Chlorofuran-2-yl-	$4\text{-}NO_2C_6H_4$	CH_3	**2e** (24)

A similar approach was used for the synthesis of the amino-isoxazole **2f**, obtained (40% yield) by using the lithiated phenyl-acetonitrile as dipolarophile instead of enolates, (Scheme 2) [33,34].
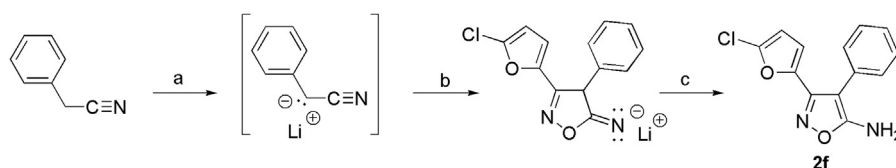
Then, 3-(5-chlorofuran-2-yl)-4-phenylisoxazol-5-amine (**2f**) was used as starting material for the preparation of **2g** and **2h**, by alkylation or acetylation reaction, respectively (Scheme 3).

Besides, we prepared 2-[3-(5-chlorofuran-2-yl)-4-phenylisoxazol-5-yl]acetic acid (**2l**), starting from 5-(bromomethyl)-3-(5-chlorofuran-2-yl)-4-phenylisoxazole (**2i**), obtained from a bromination of **P6** (Scheme 4).

P6 was reacted with NBS/AIBN to afford **2i** in 47% yield; it was transformed by NaCN/(n-Bu)₄NHSO₄ into 2-[3-(5-chlorofuran-2-yl)-4-phenylisoxazol-5-yl]acetonitrile **2j**, further converted into methyl 2-[3-(5-chlorofuran-2-yl)-4-phenylisoxazol-5-yl]acetate **2k** in the presence of *p*-TsOH and MeOH by microwave irradiation. Finally, the methyl ester **2k** was hydrolyzed with KOH/THF to afford 2-[3-(5-chlorofuran-2-yl)-4-phenylisoxazol-5-yl]acetic acid (**2l**) in good yield (Scheme 4).

3-(5-Chlorofuran-2-yl)-5-methyl-4-(4-nitrophenyl)isoxazole (**2e**) was reduced in the presence of stannous chloride and 37% hydrochloric acid to afford 4-[3-(5-chlorofuran-2-yl)-5-methylisoxazol-4-yl]benzenamine (**2m**) (Scheme 5).

2.3. Pharmacology

We have previously found [24,35] that **P6** and its analogs **P9** and **P10** inhibited platelet COX-1 and monocyte COX-2 activities with IC_{50} values (95% confidence interval) equal to 0.5 and >100 μM for **P6**, 0.05 and 1.49 μM for **P9** and 0.09 and 2.49 μM for **P10**, respectively, assessed by the *in vitro* human whole blood assay [36]. Structural features of **P6** and its analogs were used to design a new series of diarylisoxazoles (Table 1) with the aim to identify, through a SAR study, steric and electronic requirements for selective interactions between COX-1 active site and such compounds.

Initially, all compounds were screened at 50 μM on COX-1 and COX-2, and their effects on COX inhibition are summarized in Table 3. **2a**, **2c**, **2f** and **2m** showed a reasonable COX-1 inhibitory activity at the final concentration of 50 μM, compared to the "lead" compound **P6**, hence their IC_{50} values were determined (Table 3).

The obtained results showed that the substitution of the furan ring with a methoxyphenyl group lead to the selective COX-1 inhibitor **2a** (61% at 50 μM), that similarly to **P6** was inactive towards COX-2. When a methoxyphenyl was present on C_3 of the isoxazole ring and a CF_3 (**2b**) replaces a methyl group, a lower inhibition of COX-1 isoenzyme was observed, but with a little improvement of COX-2 inhibition (39% of inhibition for COX-1 and 10% for COX-2, Table 3). The oxygen on the furan ring and/or on methoxyphenyl
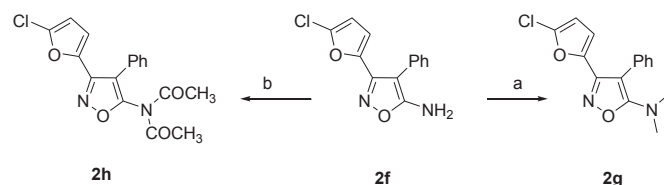
Scheme 3. Reagents and conditions: (a) paraformaldehyde, AcOH, NaBH₃CN, 25 °C; (b) Ac₂O, Py, ambient temperature.

Scheme 2. Reagents and conditions: (a) LDA, −78 °C, 2 h; (b) arylnitrile oxide; (c) sat. aq. NH₄Cl.
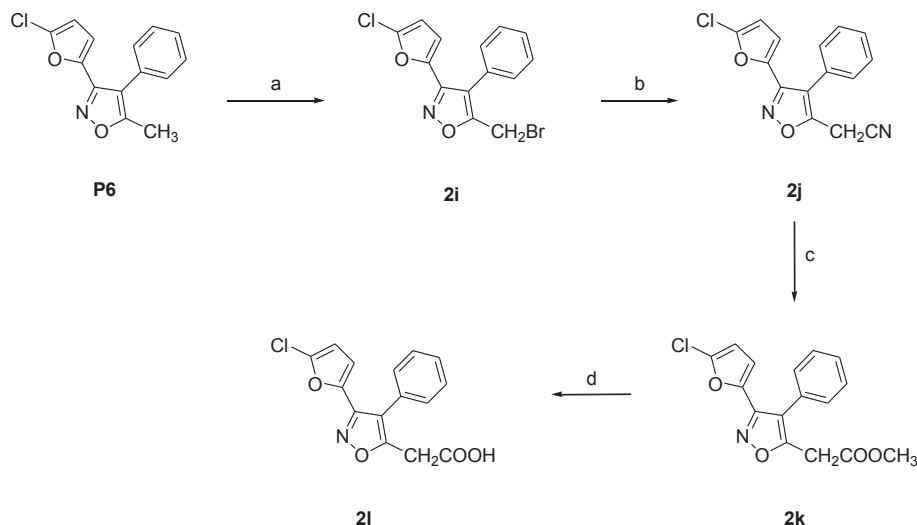
Scheme 4. Reagents and conditions: (a) NBS/AIBN, CCl$_4$; (b) NaCN/(n-Bu)$_4$NHSO$_4$; (c) MeOH/p-TsOH (MW); (d) KOH, THF.

seems to have a central role in the interaction with specific COX-1 catalytic site amino acids Trp 387 and Tyr 385 [26].

When a CH$_2$CH$_3$ replaces a methyl group as in **2c**, the COX-1 inhibitory activity was almost unchanged (COX-1 IC$_{50}$ = 30 μM) compared to **P6.**

A further alkyl chain elongation (one more methylene, **2d** in Table 3) markedly reduced COX-1 inhibitor activity (only 17% at 50 μM), whereas a 20% COX-2 inhibition was observed.

Lower COX-1 inhibition was obtained also by linking to the methylene a bromine atom (**2i**), a cyano (**2j**), and a carboxy methyl group (**2k**). They were found to be completely inactive towards COX-2 (Table 3). Based on these data, both the group size and electronic features of the substituent on the isoxazole-C$_5$ seems to play a crucial role for COX-1 inhibitory activity and selectivity.

A different result was achieved with an acidic substituent, as for **2l**, designed combining **P6** and mofezolac structural moieties (Fig. 1 and Table 1). It shown a selectivity shifted towards COX-2.

Since such different kind of substituents on C$_5$ of the isoxazole core ring were definitely detrimental for COX-1 inhibitory activity and selectivity, we also investigated the presence of nitrogen atom-containing groups, directly linked to the isoxazole or in any way present in the molecule. Hence, the amines **2f**, **2g**, as well as the amide **2h** (Table 3) were prepared. Moreover, the influence on COX-1 activity of the amine group on phenyl at isoxazole-C$_4$ (**2m**) was also studied.

Interestingly, 3-(5-chlorofuran-2-yl)-4-phenylisoxazol-5-amine (**2f**) was found to inhibit COX-1 with a potency 20 fold higher than **P6**, and this result seems particularly relevant in the exploitation of the structural modifications that can also improve the pharmacokinetic properties of such compounds (Fig. 3).

Moreover, by looking at the tertiary amine **2g** and amide **2h** behavior, the basicity of the nitrogen atom seems to be an important feature for COX selectivity and also for COX-1 inhibitory potency.

Although in previous structure–activity/selectivity relationships studies [24] the p-sulfamoyl moiety on the phenyl at isoxazole-C$_4$ was found to be detrimental for COX-1 and not COX-2 inhibitory activity, we designed the compound **2e** bearing the NO$_2$ group endowed with similar electronic effect (-M, -I).

2e was found to be not active, but it is suitable to be replaced by ^{19}F as "cold" compound or ^{18}F radionuclide, providing a radiotracer

Table 3
COX inhibitory activity of **P6** and its analogs.

Compd	Ar	R$_1$	R$_2$	COX-1 % inhibition[a] (IC$_{50}$)	COX-2 % inhibition[a] (IC$_{50}$)
2a	2-Methoxyphenyl-	C$_6$H$_5$	CH$_3$	61 (27 μM)	n.a.
2b	2-Methoxyphenyl-	C$_6$H$_5$	CF$_3$	39	10
P6	5-Chlorofuran-2-yl-	C$_6$H$_5$	CH$_3$	69 (22 μM)	10
2c	5-Chlorofuran-2-yl-	C$_6$H$_5$	CH$_2$CH$_3$	55 (30 μM)	n.a.
2d	5-Chlorofuran-2-yl-	C$_6$H$_5$	CH$_2$CH$_2$CH$_3$	17	20
2e	5-Chlorofuran-2-yl-	4-NO$_2$C$_6$H$_4$	CH$_3$	n.a.	n.a
2f	5-Chlorofuran-2-yl-	C$_6$H$_5$	NH$_2$	94 (1.1 μM)	n.a.
2g	5-Chlorofuran-2-yl-	C$_6$H$_5$	N(CH$_3$)$_2$	n.a.	n.a.
2h	5-Chlorofuran-2-yl-	C$_6$H$_5$	N(COCH$_3$)$_2$	25	n.a.
2i	5-Chlorofuran-2-yl-	C$_6$H$_5$	CH$_2$Br	35	n.a.
2j	5-Chlorofuran-2-yl-	C$_6$H$_5$	CH$_2$CN	12	n.a.
2k	5-Chlorofuran-2-yl-	C$_6$H$_5$	CH$_2$COOCH$_3$	n.a.	n.a.
2l	5-Chlorofuran-2-yl-	C$_6$H$_5$	CH$_2$COOH	32	58
2m	5-Chlorofuran-2-yl-	4-NH$_2$C$_6$H$_4$	CH$_3$	78 (4.3 μM)	38
SC-560				95 (0.077 μM)	2
Indomethacin				81 (0.099 μM)	93 (4.2 μM)
Celecoxib				40	87 (0.28 μM)

[a] Compounds were screened at a concentration of 50 μM, by a Cayman colorimetric COX (ovine) inhibitor screening assay kit. Values are the means of at least three independent measurements; n.a. = not active: no inhibitory activity was observed at the concentration of 50 μM.
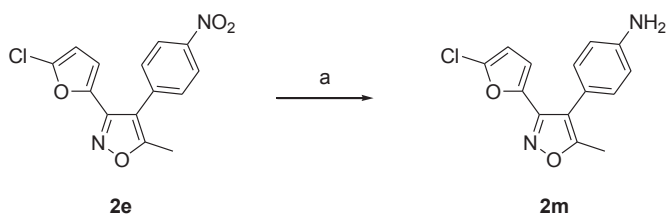
Scheme 5. Reagents and conditions: (a) SnCl$_2$/HCl, reflux, 4 h.

Fig. 3. Concentration–response curves for the inhibition of COX-1 activity by **P6** (▲; IC$_{50}$ = 22 ± 2.4 μM), **2f** (■; IC$_{50}$ = 1.1 ± 0.26 μM) and **2m** (▼; IC$_{50}$ = 4.3 ± 0.09 mm), obtained by using a colorimetric COX (ovine) assay kit. IC$_{50}$ values represent the mean ± SEM from three separate experiments.

Fig. 4. Concentration–response curve and IC$_{50}$ of **2f** by OVCAR-3 cell (8 μM ^{14}C-AA, 30 min at 37 °C).

for PET-CT imaging of physio-pathological organ in which COX-1 is a biomarker (i. e. the ovarian cancer).

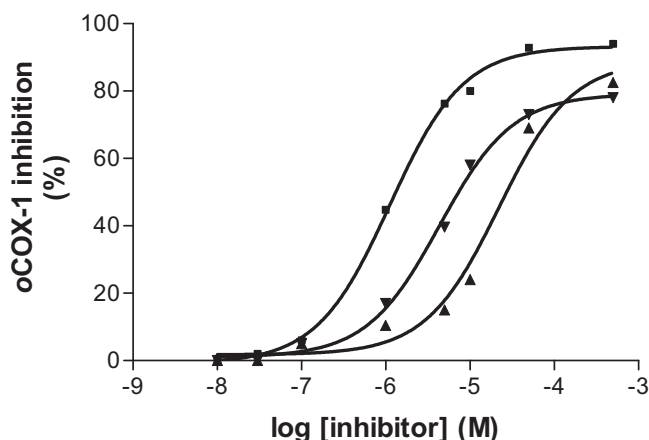Further studies are in progress to deeply investigate other substituents on this aromatic ring with quite different steric and electronic properties to definitively list determinants responsible of selective inhibition of COX-1 activity, at least for those compounds belonging to the diarylheterocycle class.

The overall obtained results suggest that (i) the oxygenated substituent on the aryl linked to the isoxazole-C$_3$ is important for COX-1 inhibition selectivity, as demonstrated by comparing the activity of **P6** and its two analogs **2a** and **2b**, lacking the furan ring replaced by a methoxyphenyl; these new selective COX-1 inhibitors could be also transformed into a PET-CT radiotracer by replacing the O^{12}CH$_3$ with O^{11}CH$_3$; (ii) the ethyl group (instead of a methyl) on isoxazole-C$_5$ of **2c**, still find enough space in the COX-1 active site, however, the selectivity is lower than **P6**; the increase of the substituent size reduces COX-1 activity and selectivity, as by comparing **P6** and propyl, bromomethyl, cyanomethyl and carboxy methyl derivatives; (iii) the carboxylic acid derivative **2l** exhibits reversal selectivity toward COX isoforms, thus giving some important indications on the different mechanism of mofezolac, **P6** and their derivate isoxazolic compounds; (iv) the introduction of a −NH$_2$ (**2f**) in place of a methyl on the isoxazole-C$_5$ gives **2f**, a new selective COX-1 inhibitor, with a COX-1 IC$_{50}$ 20 fold higher than **P6** (Table 3, Fig. 3); a similar result was obtained if the NH$_2$ is in *para* position of the phenyl on C$_4$ of isoxazole (**2m**, Fig. 3).

Finally, the inhibitory activity of the most active compound **2f** was evaluated in the OVCAR-3 cells expressing only *h*COX-1 (the second isoform is completely absent). **2f** was found to inhibit the *h*COX-1 with high potency (IC$_{50}$ = 0.58 μM, Fig. 4).

2.4. Docking studies

To get a better comprehension of the high COX-1 inhibitory potency of compounds **2f** and **2m** at a molecular level and guide further SAR studies, docking experiments were conducted using the ovine COX-1 in complex with celecoxib (PDB code: 3kk6) [37]. Docking investigations were carried out through the automated docking program GOLD 5.0.1 [38], selecting ChemPLP as a fitness function (rescoring with ChemScore) [39]. This scoring function, which uses a piecewise linear potential for hydrophobic and noncomplementary interactions and Chemscore terms for H-bonding and internal energy [40], has been recently demonstrated to be
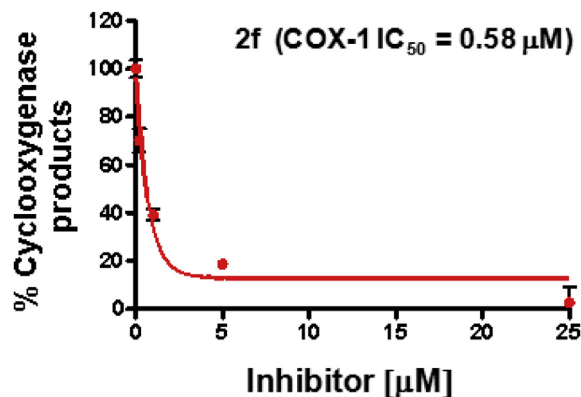
superior to the other scoring functions in GOLD for both pose prediction and virtual screening [41].

The ChemPLP-CS docking protocol was adopted in this study. In this protocol, the poses obtained with the ChemPLP function are rescored and reranked with the GOLD implementation of the ChemScore function. Several examples of successful applications of this protocol are known [27,39,42−46]. Alternative conformations of R120, Y355, S353 and S530 side chains have been previously observed in the COX crystal structures complexed with several inhibitors, highlighting the innate plasticity of the active site [47−49]. Accordingly, the side chain of R120, Y355, S353, and S530 was allowed to move during the docking experiments [50].

Docking of compounds **2f** and **2m** into COX-1 active site showed an orientation similar to that observed by us for previously published COX-1 selective isoxazoles [26]. As illustrated in Fig. 5, the ligands lie on the internal side of the constriction, at the base of the funnel-shaped entrance to the COX-1 active site. The constriction, made up of residues R120, E524, and Y355, constitutes a gate that must open and close for substrates and inhibitors to pass into or out of the COX active site [51,52]. Both O1 furan oxygen and N2 isoxazole nitrogen of compounds **2f** and **2m** is within H-bonding distance of the OH group of S353. The O1···O and N2···O atoms are separated by 2.6 Å and 2.8 Å, respectively, and display a favorable geometry for H-bonding. The furan O1 atom of the **2f** also accepts a weak H-bond from the OH group of Y355 (d$_{O1···O}$ = 3.3 Å). The O1 isoxazole oxygen of **2f** is engaged in a further H-bond with the NH$_2$ group of R120 (d$_{O1···N}$ = 2.5 Å), which plays a crucial role in binding substrates and carboxylic acid containing inhibitors. Finally, the NH$_2$ group at position 5 of isoxazole ring of compound **2f** establishes an H-bond with the S530 OH group (d$_{N5···O}$ = 2.6 Å), which adopts a "down" position during the flexible docking simulation. Unexpectedly, the NH$_2$ group at para position of phenyl ring of **2m** also interacts with S530 OH group (d$_{N···O}$ = 2.8 Å), since this residue switches in an "up" conformation. In line with our results, shifts in the position of the side chain of S530 have been observed previously in crystal structures of COX-1 and COX-2 in complex with fatty acid substrates [48,49]. It is worth noting that the extensive H-bonding network between **2f** and the COX-1 active site provides a tight anchor for the ligand, explaining its higher inhibitory potency compared to **2m**.

The phenyl ring at position 4 of isoxazole of both ligands is oriented towards the apex of the COX-1 active site and forms hydrophobic interactions with residues L352, F381, L384, Y385, W387, F518, M522 and G526. Importantly, the 5-chlorofuryl moiety of **2f** and **2m** is oriented towards the side pocket (residues 513−520) of COX-1 and makes hydrophobic contacts with residues H90, L352, I517, F518 and I523.
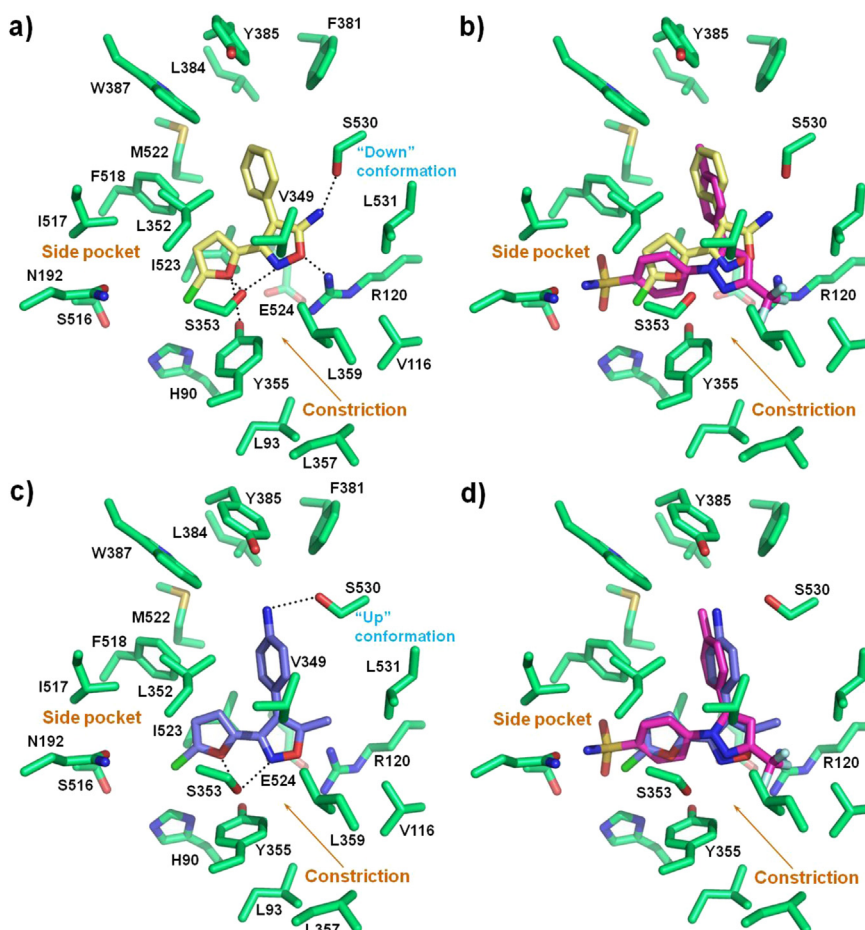
Fig. 5. Compounds **2f** (a, yellow) and **2m** (c, purple) docked into the COX-1 binding site. Docked position of compounds **2f** (b, yellow) and **2m** (d, purple) superimposed on the crystal structure position of celecoxib (magenta). Only amino acids located within 5 Å of the bound ligand are displayed and labeled. H-bonds discussed in the text are depicted as dashed black lines. (For interpretation of the references to color in this figure legend, the reader is referred to the web version of this article.)

Conformational superimposition of compounds **2f** and **2m** (from the docking simulation) and celecoxib (from the X-ray crystal structure of celecoxib/COX-1 complex), depicted in Fig. 5b and d, shows that they bind to the COX-1 active site with position and orientation very similar to that of the crystal structure of celecoxib complexed with COX-1. Whether or not this binding results in functional inhibition is more complicated to predict, as it may be related to kinetic of dissociation rather than to the stability of the complex. Given our biological results, it can be speculated that the orientation observed for compounds **2f** and **2m** in COX-1 is able to inhibit the access of arachidonic acid to the catalytic site and thus ultimately inhibit the synthesis of prostaglandins, prostacyclin, and thromboxanes.

Unfortunately, docking experiments into the binding site of COX-2 (PDB code: 6COX) [47] were not able to explain the low activity of compounds **P6**, **2f** and **2m** in inhibiting COX-2. As depicted in Fig. 6, the best solution predicted by GOLD for the representative compound **2f** was very similar to the crystallographic disposition of the selective COX-2 inhibitor SC-558 in the binding pocket of COX-2, although it did not show strong interactions nor with the COX-2 active site residues nor with the residues lining the side pocket such as H90, R513, and N192.

A mechanism proposed for diarylheterocyclic derivatives inhibition of COX-2 consists of three sequential reversible steps [53].

The first step represents the interaction of the inhibitor at the surface near the membrane-binding region of the enzyme (lobby
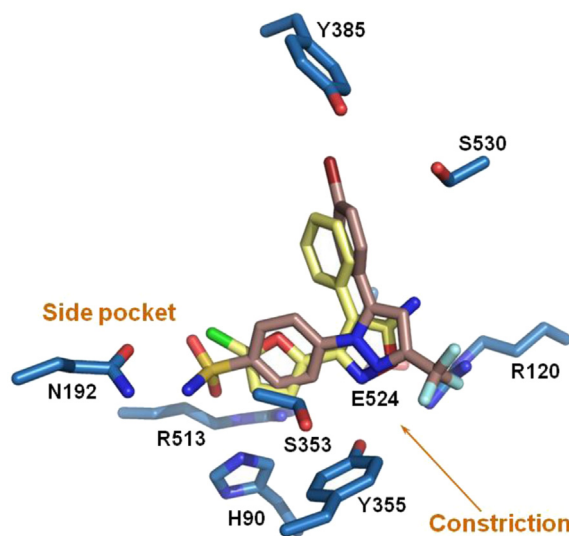

Fig. 6. The binding mode found for compound **2f** (yellow) in comparison with SC-558 (brown) from the X-ray crystal structure of SC-558/COX-2 complex (PDB code: 6COX). (For interpretation of the references to color in this figure legend, the reader is referred to the web version of this article.)

region), approximately 25 Å away from the constriction formed by R120, E524, and Y355. The second step represents the translocation of the inhibitor from the lobby to the COX-2 active site. It can be assumed that these two steps are similar for **P6**, **2f** and **2m** and several selective COX-2 inhibitors such as valdecoxib or celecoxib. However, the COX-2-selective diarylheterocycles are able to form, in a third and final step, a tightly bound enzyme inhibitor complex in the active site and a side pocket of COX-2 due to their phenyl-sulfonamide or a phenylsulfamoyl group. We suppose that compounds **P6**, **2f** and **2m**, lacking the sulfonamide or sulfamoyl group, cannot form this tight complex due to the absence of any profitable interaction, and are easily released from the binding pocket of COX-2.

3. Conclusions

All the new compounds have been prepared in good yields by developing suitable, efficient and versatile synthetic methodologies [34].

Many structural modifications have been proposed during this investigation, that allowed us also to find out the rationale of the molecular basis of some selective interactions between COX-1 enzyme and **P6** and/or its analogs: SAR studies have contributed to define the importance of the oxygen of substituent linked to isoxazole-C$_3$ for the inhibition of COX-1 activity and COX selectivity. A number of these compounds are precursors of possible radio-labelled selective COX-1 inhibitors to be used as PET-CT radiotracers in ovarian cancer diagnosis. In addition, the substituent size on C$_5$ of isoxazole ring seems to be determinant for potency and selectivity in COX-1 inhibition. The substitution of methyl with an amino group on that position increases COX-1 inhibitory activity and selectivity (**2f**) compared to **P6**. Low or no activity at all was instead observed for its *N,N*-dialkyl (**2g**) and *N,N*-diacetyl (**2h**) derivatives. Molecular docking studies of the most active inhibitor **2f** into the active site of COX-1 suggest critical interactions between the inhibitor and the constriction residues R120 and Y355 at the base of the active site, as well as an interaction with S530 at the top of the pocket.

The data herein reported suggest some molecular determinants necessary to design new diarylisoxazoles as inhibitors of cyclo-oxygenases, mainly COX-1. A full pharmacological characterization of some of the above compounds will be carried out in order to prove their pharmacokinetic properties, metabolic stability and the possibility of their use as diagnostic tools, analgesics, anti-inflammatories, antiproliferative and chemopreventive drugs.

Further studies are in progress aimed to fine tune the isoxazole structure to clarify at atomic level, including X-ray of the COX-1-inhibitor complexes, the reasons of the marked inhibitory activity and selectivity of the novel series of isoxazoles above described.

4. Experimental protocols

4.1. Chemistry

4.1.1. General methods

Melting points taken on electrothermal apparatus were uncorrected. ^{1}H NMR and ^{13}C NMR spectra were recorded on a Varian-Mercury 300 MHz, on a Varian-Inova-400 MHz spectrometer, on a Bruker-Aspect 3000 console 500 MHz spectrometer and chemical shifts are reported in parts per million (δ). ^{19}F NMR spectra were recorded by using CFCl$_3$ as internal standard. Absolute values of the coupling constant are reported. FT-IR spectra were recorded on a Perkin—Elmer 681 spectrometer. GC analyses were performed by using an HP1 column (methyl siloxane; 30 m × 0.32 mm × 0.25 μm film thickness) on an HP 6890 model, Series II. Thin-layer chromatography (TLC) was performed on silica gel sheets with

fluorescent indicator, the spots on the TLC were observed under ultraviolet light or were visualized by I$_2$ vapor exposure. Column chromatography was conducted by using silica gel 60 with a particle size distribution 40—63 μm and 230-400 ASTM. GC—MS analyses were performed on an HP 5995C model. MS-ESI analyses were performed on Agilent 1100 LC/MSD trap system VL. All synthesized compounds were analyzed by HPLC analysis, performed on an Agilent 1260 Infinity instrument equipped with a 1260 DAD VL+ detector on a column Poroshell 120 EC-18 3 × 50 mm 2.7Micron (eluent CH$_3$CN/H$_2$O = 70/30; λ = 280 nm), and their purity is higher than 95%.

4.1.2. Materials

Tetrahydrofuran from commercial source was purified by distillation (twice) from sodium wire under nitrogen. Dichloromethane from commercial source was purified by distillation from CaH$_2$ under nitrogen atmosphere. Dimethylformamide from commercial source was purified by distillation from CaH$_2$ under reduced pressure. Standardized (2.5 M) *n*-butyllithium in hexanes was purchased from Aldrich Chemical Co. and its titration was performed with *N*-pivaloyl-*o*-toluidine [54]. Diisopropylamine from commercial source was purified by distillation from CaH$_2$ under reduced pressure and nitrogen atmosphere. All other chemicals and solvents were commercial grade further purified by distillation or crystallization prior to use. Arylnitrile oxides were prepared from aldehydes through their conversion into the corresponding oximes and then into benzohydroximinoyl chlorides [31,32,55,56]. These were finally converted into nitrile oxides by treatment with Et$_3$N, followed by *vacuum* filtration of Et$_3$N·HCl from the solution. Oximes [24,57—59], prepared from reaction of aldehydes/EtOH and NH$_2$OH·HCl/aq.NaOH, had analytical and spectroscopic data identical to those previously reported or commercially available.

4.1.3. General procedure for the synthesis of 3,4-diarylisoxazoles (2a—e)

A solution of the 3-aryl-2-propanones **1a—e** (0.6 mmol) in THF (3 mL) was dropwise added to a suspension of NaH (95% w/w, 1.2 mmol) in THF (6 mL) kept at 0 °C under nitrogen atmosphere, using a nitrogen-flushed, three necked flask equipped with a magnetic stirrer, a nitrogen inlet and two dropping funnels. After the yellow mixture had been stirred for 1 h, a solution of arylnitrile oxide (0.6 mmol) in THF (3 mL) was added. The reaction mixture was allowed to reach room temperature, stirred overnight and then quenched by adding aqueous NH$_4$Cl solution. The reaction products were extracted three times with ethyl acetate. The combined organic phases were dried over anhydrous Na$_2$SO$_4$ and then evaporated under vacuum. Column chromatography (silica gel, petroleum ether:ethyl acetate = 19/1) of the residue affords the 3,4-diarylisoxazoles **(2a—e)** in 21—60% yields (Table 2). 3-(5-Chlorofuran-2-yl)-4-phenyl-5-methylisoxazole (P6) spectroscopic and pharmacological data have been previously reported [24,57].

4.1.3.1. 3-(2-Methoxyphenyl)-5-methyl-4-phenylisoxazole **(2a)**. 43% yield (30 mg). Mp 90—92 °C (Et$_2$O), white crystals. FT-IR (KBr): 3050, 2925, 1604, 1496, 1466, 1411, 1249, 1103, 1018, 899, 798, 755, 699 cm^{-1}. ^{1}H NMR (400 MHz, CDCl$_3$, δ): 7.47—7.45(m, 1H, aromatic proton); 7.41—7.36 (m, 1H, aromatic proton); 7.31—7.22 (m, 3H, aromatic protons); 7.10—7.07 (m, 2H, aromatic protons); 7.03—6.98 (m, 1H, aromatic proton); 6.80 (d, 1H, *J* = 8.3 Hz, aromatic proton); 3.29 (s, 3H), 2.52 (s, 3H). ^{13}C NMR (100 MHz, CDCl$_3$, δ): 165.1, 160.2, 157.0, 131.5, 131.1, 130.96, 128.24, 128.22, 126.9, 120.7, 118.5, 117.2, 111.2, 54.8, 11.7. GC—MS (70 eV) *m/z* (int.rel.): 265 (M$^+$, 100), 250 (38), 223 (35), 222 (18), 208 (23), 207 (18), 152 (8), 115 (7), 104 (6), 103 (8), 89 (11), 77 (8), 63 (6).

*4.1.3.2. 3-(2-Methoxyphenyl)-4-phenyl-5-(trifluoromethyl)isoxazole (**2b**).* 43 % yield. Mp 44–46 °C (hexane), white powder. FT-IR (KBr): 3062, 2963, 2926, 2850, 1606, 1584, 1515, 1496, 1468, 1448, 1437, 1412, 1324, 1260, 1194, 1089, 1046, 1024, 953, 798 754, 698 cm^{-1}. ^{1}H NMR (400 MHz, CDCl$_3$, δ): 7.47–7.39 (m, 2H, aromatic protons); 7.32–7.28 (m, 3H, aromatic protons); 7.16–7.12 (m, 2H, aromatic protons); 7.06–7.01 (m, 1H, aromatic proton); 6.78 (d, 1H, $J = 8.2$ Hz, aromatic proton); 3.26 (s, 3H). ^{13}C NMR (100 MHz, CDCl$_3$, δ): 161.7, 156.9, 131.9, 131.2, 128.6 (m), 128.4, 128.1 (2C), 127.7, 120.8, 118.6 (q, ^{1}J$_{C-F}$= 271 Hz), 116.4, 111.2, 54.7. ^{19}F NMR (376 MHz, CDCl$_3$, δ): −65.6 (s). GC–MS (70 eV) m/z (int.rel.): 319 (M$^+$, 100), 251 (17), 250 (94), 235 (10), 220 (9), 207 (18), 178 (8), 115 (13), 89 (19), 77 (8), 63 (8), 51 (33).

*4.1.3.3. 3-(5-Chlorofuran-2-yl)-5-ethyl-4-phenylisoxazole (**2c**).* 46% yield. Mp 82–85 °C, yellow solid. FT-IR (KBr): 3137, 3063, 2964, 2940, 1628, 1594, 1518, 1427, 1412, 1261, 1204, 1094, 1017, 864, 798, 711 cm^{-1}. ^{1}H NMR (400 MHz, CDCl$_3$, δ): 7.45–7.41 (m, 3H, aromatic protons), 7.29–7.26 (m, 2H, aromatic protons); 6.20 (d, 1H, $J = 3.3$ Hz); 6.12 (d, 1H, $J = 3.3$ Hz); 2.73 (q, 2H, $J = 7.5$ Hz); 1.26 (t, 3H, $J = 7.5$ Hz). ^{13}C NMR (100 MHz, CDCl$_3$, δ): 171.4, 152.2, 143.6, 138.3, 130.0, 129.5, 128.7, 128.39, 113.9, 113.5, 107.8, 19.1, 12.2. GC–MS (70 eV) m/z (rel.int.): 275 [M(^{37}Cl)$^+$, 15], 273 [M(^{35}Cl)$^+$, 44], 219 (34), 218 (16), 217 (100), 188 (8), 154 (24), 153 (17), 152 (9), 129 (8), 127 (14), 89 (11), 77 (6), 57 (12).

*4.1.3.4. 3-(5-Chlorofuran-2-yl)-4-phenyl-5-propylisoxazole (**2d**).* 21% yield. Yellow oil. FT-IR (neat): 3058, 2964, 2933, 2874, 1627, 1595, 1520, 1497, 1436, 1416, 1261, 1207, 1135, 1093, 1018, 987, 942, 900, 794, 771, 702 cm^{-1}. ^{1}H NMR (400 MHz, CDCl$_3$, δ): 7.47–7.43 (m, 3H, aromatic protons), 7.29–7.26 (m, 2H, aromatic protons); 6.18 (d, 1H, $J = 3.3$ Hz); 6.12 (d, 1H, $J = 3.3$ Hz); 2.68 (t, 2H, $J = 7.5$ Hz); 2.68 (sextet, 2H, $J = 7.5$ Hz); 0.93 (t, 3H, $J = 7.5$ Hz). ^{13}C NMR (100 MHz, CDCl$_3$, δ): 170.4, 152.2, 143.6, 138.3, 130.1, 129.5, 128.7, 128.3, 113.5, 107.8, 94.4, 27.4, 21.1, 13.6. GC–MS (70 eV) m/z (rel.int.): 289 [M(^{37}Cl)$^+$, 11], 287 [M(^{35}Cl)$^+$, 32], 219 (31), 218 (15), 217 (100), 188 (7), 154 (20), 153 (17), 127 (45), 89 (17), 77 (13), 71 (29), 43 (39).

*4.1.3.5. 3-(5-Chlorofuran-2-yl)-5-methyl-4-(4-nitrophenyl)isoxazole (**2e**).* 24 % yield. Mp 153–155 °C (hexane), white powder. FT-IR (KBr): 3144, 3103, 3071, 2929, 2851, 1628, 1601, 1559, 1519, 1441, 1419, 1345, 1239, 1204, 1136, 1105, 1019, 988, 896, 867, 853, 797, 761, 730, 709, 688, 560, 513 cm^{-1}. ^{1}H NMR (400 MHz, CDCl$_3$, δ): 8.32 (d, 2H, $J = 8.3$ Hz, aromatic protons); 7.49 (d, 2H, $J = 8.3$ Hz, aromatic protons); 6.49 (d, 1H, $J = 3.5$ Hz); 6.21 (d, 1H, $J = 3.5$ Hz); 2.45 (s, 3H). ^{13}C NMR (100 MHz, CDCl$_3$, δ): 167.7, 151.8, 147.6, 142.7, 138.8, 136.5, 130.8, 123.9, 113.7, 113.3, 108.1, 11.4. GC–MS (70 eV) m/z (int.rel.): 306 (M(^{37}Cl)$^+$, 15), 304 (M(^{35}Cl)$^+$, 45), 264 (33), 262 (100), 245 (7), 217 (13), 215 (15), 199 (7), 188 (9), 187 (12), 152 (9), 89 (16), 73 (8), 63 (6), 43 (52).

*4.1.4. General procedure for the synthesis of 3-(5-chlorofuran-2-yl)-4-phenylisoxazol-5-amine (**2f**)*

A 2.5 M solution of *n*-butyllithium in hexane (1.068 mL, 2.67 mmol) was added to diisopropylamine (0.413 mL, 2.97 mmol) in anhydrous THF (10 mL) kept at 0 °C under nitrogen atmosphere, using a nitrogen-flushed, three necked flask equipped with a magnetic stirrer, a nitrogen inlet and two dropping funnels. After the mixture had been stirred for 15 min, the reaction mixture was kept at −78 °C, then phenylacetonitrile (0.300 mL, 2.23 mmol) was dropwise added. The yellow reaction mixture was stirred at 0 °C for 1 h, then the solution of arylnitrile oxide (2.23 mmol) in anhydrous THF (10 mL) was added [24]. The orange-colored reaction mixture was allowed to reach room temperature and stirred overnight. After quenching by addition of aqueous NH$_4$Cl solution, the

reaction products were extracted three times with ethyl acetate. The organic phase was dried over anhydrous Na$_2$SO$_4$ and then the solvent evaporated under vacuum. Column chromatography (silica gel, petroleum ether:ethyl acetate = from 20/1 to 8/2) of the residue affords the 5-(chlorofuran-2-yl)-4-phenylisoxazol-5-amine (105 mg) in 40% yield.

*4.1.4.1. 3-(5-Chlorofuran-2-yl)-4-phenylisoxazol-5-amine (**2f**).* Mp 138.5–141 °C (EtOAc/hexane). FT-IR (KBr): 3460, 3402.6, 3115, 2927, 1643, 1518, 1506, 1474, 1413, 1318, 1208, 1148, 1020, 988, 940, 896, 786, 699 cm^{-1}. ^{1}H NMR (400 MHz, CDCl$_3$, δ): 7.45–7.41 (m, 2H, aromatic protons); 7.39–7.31 (m, 3H, aromatic protons); 6.36 (d, $J = 3.5$ Hz, 1H, furyl proton); 6.14 (d, $J = 3.5$ Hz, 1H, furyl proton); 4.56 (bs, 2H, NH$_2$: exchange with D$_2$O). ^{13}C NMR (100 MHz, CDCl$_3$, δ): 165.8, 153.1, 143.9, 138.4, 130.0, 129.8, 129.3, 128.1, 113.7, 108.1, 93.5. GC–MS (70 eV) m/z (rel.int.): 262 [M (^{37}Cl)$^+$, 11], 260 [M (^{35}Cl)$^+$, 31], 225 (6), 218 (20), 216 (54), 197 (8), 188 (13), 180 (20), 154 (15), 153 (16), 152 (32), 131 (31), 129 (100), 127 (16), 115 (10), 113 (21), 105 (28), 104 (27), 103 (13), 101 (26), 94 (42), 89 (14), 85 (18), 77 (54), 76 (11), 63 (15), 51 (14).

*4.1.5. Synthesis of 3-(5-chlorofuran-2-yl)-N,N-dimethyl-4-phenylisoxazol-5-amine (**2g**)*

To a stirred mixture of 3-(5-chlorofuran-2-yl)-4-phenylisoxazol-5-amine (**2f**) (475 mg, 1.83 mmol) and paraformaldehyde (548 mg, 18.27 mmol) in AcOH (5 mL) at 25 °C under nitrogen, sodium cyanoborohydride was added (574 mg, 9.14 mmol). The reaction mixture was kept under stirring for 3 days. EtOAc and saturated aqueous NaHCO$_3$ solution (10 mL) were added. The two phases were separated and the aqueous layer was extracted three times with EtOAc. The combined organic extracts were dried over anhydrous Na$_2$SO$_4$ and the solvent removed under reduced pressure. Column chromatography (silica gel, mobile phase: petroleum ether/ethyl acetate = 9:1) of the residue afforded the product with 25% yield [60].

*4.1.5.1. 3-(5-Chlorofuran-2-yl)-N,N-dimethyl-4-phenylisoxazol-5-amine (**2g**).* Mp 89.8–91 °C (EtOAc/hexane). FT-IR (KBr): 3109, 3054, 2927, 2875, 1626, 1600, 1515, 1484, 1423, 1409, 1324, 1247, 1206, 1026, 820, 772, 739, 701, 515 cm^{-1}. ^{1}H NMR (400 MHz, CDCl$_3$, δ): 7.39–7.37 (m, 3H, aromatic protons); 7.32–7.30 (m, 2H, aromatic protons); 6.04 (d, $J = 3.5$ Hz, 1H, furyl proton); 6.86 (d, $J = 3.5$ Hz, 1H, furyl proton); 2.84 (s, 6H, CH$_3$). ^{13}C NMR (100 MHz, CDCl$_3$, δ): 162.9, 150.5, 140.5, 134.0, 128.2, 127.4, 124.6, 124.2, 109.3, 103.8, 87.9, 35.6. GC–MS (70 eV) m/z (rel.int.): 290 [M (^{37}Cl)$^+$, 18], 288 [M (^{35}Cl)$^+$, 44], 253 (27), 188 (11), 145 (100), 139 (10), 129 (13), 127 (22), 105 (10), 89 (22), 77 (12), 76 (11), 72 (31), 64 (18), 63 (12).

*4.1.6. Synthesis of N-acetyl-N-(3-(5-chlorofuran-2-yl)-4-phenylisoxazol-5-yl)acetamide (**2h**)*

To a solution of 3-(5-chlorofuran-2-yl)-4-phenylisoxazol-5-amine (**2f**) (458 mg, 1.76 mmol) and pyridine (0.264 mL, 3.28 mmol), Ac$_2$O (0.41 mL, 4.40 mmol) was added. The reaction mixture was kept under stirring for 20 h at r.t. EtOAc and saturated aqueous NaHCO$_3$ solution (10 mL) were added. The two phases were separated and the aqueous layer was extracted three times with EtOAc. The combined organic extracts were dried over anhydrous Na$_2$SO$_4$ and the solvent removed under reduced pressure. Column chromatography (silica gel, mobile phase: petroleum ether/ethyl acetate = 10:1) of the residue afforded the product with 30% yield.

*4.1.6.1. N-Acetyl-N-[3-(5-chlorofuran-2-yl)-4-phenylisoxazol-5-yl] acetamide (**2h**).* Mp 98–100 °C (EtOAc/hexane). FT-IR (KBr): 3142, 3021, 2942, 1740, 1651, 1600, 1519, 1498, 1429, 1367, 1256, 1208, 1146, 1074, 1036, 1003, 994, 984, 942, 897, 799, 769, 703, 678 cm^{-1}.

^{1}H NMR (400 MHz, CDCl$_3$, δ): 7.47–7.44 (m, 3H, aromatic protons); 7.28–7.26 (m, 2H, aromatic protons); 6.34 (d, J = 3.5 Hz, 1H, furyl proton); 6.18 (d, J = 3.5 Hz, 1H, furyl proton); 2.30 (s, 6H, CH$_3$). ^{13}C NMR (100 MHz, CDCl$_3$, δ): 170.9, 158.4, 153.9, 142.4, 139.3, 129.5, 129.2, 129.0, 126.7, 114.8, 114.7, 108.2, 25.6. GC–MS (70 eV) m/z (rel.int.): 346 [M (^{37}Cl)$^+$, 4], 344 [M (^{35}Cl)$^+$, 12], 304 (25), 303 (13), 302 (73), 267 (13), 262 (13), 261 (37), 260 (37), 259 (100), 231 (10), 225 (32), 224 (15), 218 (20), 197 (27), 196 (17), 190 (14), 179 (19), 175 (12), 168 (14), 164 (13), 162 (10), 155 (45), 154 (26), 145 (10), 144 (10), 139 (15), 127 (36), 126 (12), 119 (14), 117 (64), 105 (25), 89 (13), 77 (29), 64 (7), 63 (7), 51 (9), 43 (57). ESI-MS: m/z (%): 367 [M + Na]$^+$ (100); MS–MS (367): 325 (100), 282 (62), 284 (27), 248 (23), 226 (13), 225 (10).

4.1.7. Synthesis of 5-(bromomethyl)-3-(5-chlorofuran-2-yl)-4-phenylisoxazole (2i)

To a solution of 3-(5-chlorofuran-2-yl)-4-phenyl-5-methyl-isoxazole (0.500 g, 1.930 mmol) (P6) dissolved in anhydrous CCl$_4$ (10 mL), contained in a argon-flushed, three necked flask equipped with a magnetic stirrer *N*-bromosuccinimide (412 mg, 2.32 mmol) was added. Then, AIBN (0.158 g, 0.965 mmol) was added, and the obtained suspension was stirred overnight at room temperature. The reaction mixture was kept under reflux for 4 h, and then water and ethyl acetate were added. The two phases were separated and the aqueous layer was extracted three times with ethyl acetate. The combined organic extracts washed with brine and KOH (1 M), were dried over anhydrous Na$_2$SO$_4$ and the solvent evaporated under vacuum. Column chromatography (silica gel, petroleum ether:ethyl acetate = 10/1) of the residue affords the 5-(bromo-methyl)-3-(5-chlorofuran-2-yl)-4-phenylisoxazole (2i) in 47% yield as a solid.

4.1.7.1. 5-(Bromomethyl)-3-(5-chlorofuran-2-yl)-4-phenylisoxazole (2i).
Mp 88.5–90.3 °C (hexane). FT-IR (neat): 3137, 3065, 2924, 1628, 1515, 1435, 1410, 1266, 1206, 1136, 1096, 1017, 1009, 988, 948, 942, 902, 789, 774, 704 cm^{-1}. ^{1}H NMR (400 MHz, CDCl$_3$, δ): 7.50–7.46 (m, 3H, aromatic protons); 7.39–7.36 (m, 2H, aromatic protons); 6.31 (d, J = 3.5 Hz, 1H, furyl proton); 6.15 (d, J = 3.5 Hz, 1H, furyl proton); 4.38 (s, 2H, CH$_2$). ^{13}C NMR (75 MHz, CDCl$_3$, δ): 164.6, 152.8, 143.1, 139.1, 130.2, 129.9, 129.3, 129.2, 117.2, 114.4, 108.3, 17.8. GC–MS (70 eV) m/z (rel. int.): 341 [M(^{81}Br, ^{37}Cl)$^+$, 26], 339 [M (^{79}Br, ^{37}Cl)$^+$, 100], 337 [M (^{79}Br, ^{35}Cl)$^+$, 78], 258 (22), 246 (11), 244 (33), 232 (12), 230 (35), 223 (14), 219 (17), 218 (13), 217 (54), 216 (19), 190 (16), 188 (46), 167 (25), 166 (16), 163 (12), 154 (18), 153 (29), 152 (28), 140 (10), 139 (18), 129 (66), 128 (11), 127 (24), 115 (34), 103 (19), 102 (13), 91 (28), 89 (38), 77 (18), 75 (13), 73 (17), 63 (12), 51 (9).

4.1.8. Synthesis of 2-[3-(5-chlorofuran-2-yl)-4-phenylisoxazol-5-yl]acetonitrile (2j)

To a solution of 5-(bromomethyl)-3-(5-chlorofuran-2-yl)-4-phenylisoxazole (2i) (1.520 g, 4.51 mmol) in dichloromethane (61 mL), tetrabutylammonium hydrogen sulfate (3.06 g, 9.02 mmol) and a solution of NaCN (0.265 g, 5.41 mmol) in water (61 mL) were added, and the suspension kept under stirring at room temperature for 5 h. Then, the two phases were separated and aqueous layer was extracted three times with dichloromethane. The combined organic extracts, washed with brine, were dried over anhydrous Na$_2$SO$_4$ and the solvent evaporated under vacuum. Column chromatography (silica gel, petroleum ether:ethyl acetate = 20/1) of the residue affords 1.050 g of 2-[3-(5-chlorofuran-2-yl)-4-phenylisoxazol-5-yl]acetonitrile in 80% yield.

4.1.8.1. 2-[3-(5-Chlorofuran-2-yl)-4-phenylisoxazol-5-yl]acetonitrile (2j).
Dec 170.5 °C (hexane) FT-IR (neat): 3050, 2959, 2918, 2850,

2260, 1631, 1518, 1466, 1412, 1261, 1207, 1096, 1018, 942, 798, 729, 701 cm^{-1}. ^{1}H NMR (400 MHz, CDCl$_3$, δ): 7.52–7.49 (m, 3H, aromatic protons); 7.35–7.31 (m, 2H, aromatic protons); 6.29 (d, J = 3.5 Hz, 1H, furyl proton); 6.16 (d, J = 3.5 Hz, 1H, furyl proton); 3.83 (s, 2H, CH$_2$). ^{13}C NMR (75 MHz, CDCl$_3$, δ): 157.7, 153.0, 142.6, 139.4, 130.1, 129.7, 129.5, 127.4, 117.7, 114.8, 113.6, 108.4, 15.4. GC–MS (70 eV) m/z (rel.int.): 286 [M (^{37}Cl)$^+$, 34], 285 (18), 284 [M (^{35}Cl)$^+$, 100], 256 (15), 249 (36), 246 (10), 244 (29), 222 (6), 221 (34), 218 (9), 216 (27), 215 (10), 193 (20), 190 (24), 189 (14), 188 (75), 187 (17), 180 (12), 154 (10), 153 (42), 152 (40), 129 (61), 128 (18), 127 (27), 126 (11), 115 (12), 102 (9), 101 (8), 91 (15), 89 (54), 77 (18), 75 (15), 73 (15), 63 (16), 51 (8).

4.1.9. Synthesis of methyl 2-[3-(5-chlorofuran-2-yl)-4-phenylisoxazol-5-yl]acetate (2k)

2-[3-(5-Chlorofuran-2-yl)-4-phenylisoxazol-5-yl]acetonitrile (2j) (0.057 g, 0.179 mmol) and *p*-toluenesulfonic acid (*p*-TsOH) (0.035 g, 0.179 mmol) were dissolved in MeOH (4 mL) in a glass vessel with Teflon stoppers, and heated during 20 min at 100 °C, using a microwave apparatus at 300 W. Then, to the resulting solution, water (10 mL) and EtOAc (10 mL) were added. The two phases were separated and aqueous layer was extracted three times with EtOAc. The combined organic extracts were dried over anhydrous Na$_2$SO$_4$ and the solvent evaporated under vacuum. Column chromatography (silica gel, petroleum ether:ethyl acetate = 10/1) of the residue affords 0.040 g of methyl 2-(3-(5-chlorofuran-2-yl)-4-phenylisoxazol-5-yl)acetate in 88% yield.

4.1.9.1. Methyl 2-[3-(5-chlorofuran-2-yl)-4-phenylisoxazol-5-yl]acetate (2k).
Yellow oil. FT-IR (neat): 3140, 2955, 2923, 2852, 1743, 1635, 1597, 1518, 1497, 1436, 1414, 1332, 1295, 1260, 1206, 1177, 1131, 1017, 987, 942, 898, 796, 772, 701, 680 cm^{-1}. ^{1}H NMR (400 MHz, CDCl$_3$, δ): 7.46–7.43 (m, 3H, aromatic protons); 7.33–7.30 (m, 2H, aromatic protons); 6.26 (d, J = 3.2 Hz, 1H, furyl proton); 6.14 (d, J = 3.2 Hz, 1H, furyl proton); 3.75 (s, 2H, CH$_2$); 3.71 (s, 3H, CH$_3$). ^{13}C NMR (100 MHz, CDCl$_3$, δ): 167.7, 162.3, 152.4, 143.1, 138.6, 129.9, 128.8, 128.7, 116.9, 113.9, 107.9 52.6, 31.4. GC–MS (70 eV) m/z (rel.int.): 319 [M (^{37}Cl)$^+$, 26], 318 (13), 317 [M (^{35}Cl)$^+$, 76], 277 (6), 275 (19), 247 (16), 244 (23), 219 (33), 218 (18), 217 (100), 216 (14), 190 (7), 188 (22), 154 (48), 153 (19), 152 (15), 129 (23), 128 (9), 127 (19), 115 (15), 103 (9), 102 (10), 101 (11), 91 (12), 77 (14), 59 (14), 51 (4).

4.1.10. Synthesis of 2-[3-(5-chlorofuran-2-yl)-4-phenylisoxazol-5-yl]acetic acid (2l)

KOH (1.340 mmol) in H$_2$O (7 mL) was added to the methyl 2-[3-(5-chlorofuran-2-yl)-4-phenylisoxazol-5-yl]acetate (2k) (211 mg, 0.670 mmol) in THF (8 mL). The reaction mixture was stirred overnight at room temperature. Then, THF was distilled under reduced pressure and ethyl ether was added to the residue. The two phases were separated. 10% HCl was added to the aqueous phase till pH < 5, and the product extracted three times with ethyl ether. The combined organic phases were dried over anhydrous Na$_2$SO$_4$ and then the solvent was evaporated under reduced pressure. The residue recrystallized from CHCl$_3$/hexane afforded the pure products as a pale yellow solid (60% yield).

4.1.10.1. 2-[3-(5-Chlorofuran-2-yl)-4-phenylisoxazol-5-yl]acetic acid (2l).
Mp 61–63 °C (CHCl$_3$/hexane). FT-IR (neat): 3600–3000, 2927, 2590, 1722, 1635, 1519, 1436, 1414, 1292, 1208, 1156, 1134, 1020, 989, 942, 898, 791, 771, 703 cm^{-1}. ^{1}H NMR (400 MHz, CDCl$_3$, δ): 9.10–8.90 (bs, 1H, OH: exchanges with D$_2$O); 7.47–7.41 (m, 3H, aromatic protons); 7.34–7.31 (m, 2H, aromatic protons); 6.27 (d, J = 3.4 Hz, 1H, furyl proton); 6.14 (d, J = 3.4 Hz, 1H, furyl proton); 3.79 (s, 2H, CH$_2$). ^{13}C NMR (100 MHz, CDCl$_3$, δ): 173.0, 161.7, 152.4, 142.9, 138.8,

129.9, 128.95, 128.91, 128.2, 117.3, 114.1, 108.0, 31.2. ESI-MS: *m/z* (%): 326 [M + Na]$^+$ (100); 304 [M + H]$^+$ (100); MS–MS (326): 284 (15), 282 (100), 246 (83).

4.1.11. Synthesis of 4-[3-(5-chlorofuran-2-yl)-5-methylisoxazol-4-yl]benzenamine (**2m**)

To a stirred mixture of stannous chloride (298 mg, 1.32 mmol) in hydrochloric acid 37% (1 mL) at 25 °C, a solution of 3-(5-chlorofuran-2-yl)-5-methyl-4-(4-nitrophenyl)isoxazole (**2e**) (100 mg, 0.33 mmol) dissolved in absolute EtOH (8 mL) was added. The reaction mixture was kept under reflux for 4 h. 10% NaOH (10 mL) was added to the reaction mixture till pH = 12, and the aqueous phase extracted three times with EtOAc. The combined organic extracts were dried over anhydrous Na$_2$SO$_4$ and the solvent removed under reduced pressure. The residue afforded the product with 98% yield.

4.1.11.1. 4-[3-(5-Chlorofuran-2-yl)-5-methylisoxazol-4-yl]benzenamine (**2m**).
Mp 132–134 °C (EtOAc/hexane). FT-IR (KBr): 3486, 3386, 3143, 3032, 2924, 1626, 1520, 1441, 1411, 1298, 1234, 1204, 1180, 1136, 1016, 988, 941, 899, 838, 799, 739, 565, 518 cm^{-1}. ^{1}H NMR (300 MHz, CDCl$_3$, δ): 7.26 (bs, 2H, NH$_2$: exchange with D$_2$O); 7.04 (d, 2H, *J* = 8.4 Hz, aromatic protons); 6.74 (d, 2H, *J* = 8.4 Hz, aromatic protons); 6.28 (d, 1H, *J* = 3.5 Hz, furyl proton); 6.13 (d, 1H, *J* = 3.5 Hz, furyl proton); 2.35 (s, 3H). ^{13}C NMR (100 MHz, CDCl$_3$, δ): 166.8, 152.7, 146.8, 144.1, 138.4, 131.2, 119.1, 115.4, 114.9, 113.8, 108.1, 11.4. GC–MS (70 eV) *m/z* (rel.int.): 276 [M (^{37}Cl)$^+$, 34], 274 [M (^{35}Cl)$^+$, 100], 234 (13), 233 (19), 232 (40), 231 (48), 203 (15), 169 (19), 168 (29), 159 (26), 144 (29), 142 (12), 119 (29), 118 (21), 117 (10), 113 (10), 89 (11), 77 (7), 65 (6), 63 (6), 51 (4), 43 (14).

4.2. Biology

4.2.1. Inhibition studies of cyclooxygenase activity

The final compounds were evaluated for their ability to inhibit ovine COX-1/COX-2 enzyme (percent inhibition at 50 μM). The inhibition of the enzyme was determined using a colorimetric COX (ovine) inhibitor screening assay kit (Catalog No. 760111, Cayman Chemicals, Ann Arbor, MI, USA) following the manufacturer's instructions.

COX is a bifunctional enzyme exhibiting both cyclooxygenase and peroxidase activities. The cyclooxygenase component catalyzes the conversion of arachidonic acid into a hydroperoxide (PGG$_2$), and the peroxidase component catalyzes the reduction of endoperoxidase into the corresponding alcohol (PGH$_2$), the precursor of PGs, thromboxanes, and prostacyclin. The Colorimetric COX Inhibitor Screening Assay measures the peroxidase component of the cyclooxygenases. The peroxidase activity is assayed colorimetrically by monitoring the appearance of oxidized *N,N,N′,N′*-tetramethyl-*p*-phenylenediamine (TMPD) at 590 nm. Stock solutions of test compounds were dissolved in a minimum volume of DMSO.

4.2.2. In vitro OVCAR-3 cell assay

Human ovarian adenocarcinoma cells, OVCAR-3, passage 13–17, mycoplasma negative by PCR detection method (Sigma VenorGem) were grown in RPMI 1640 (Invitrogen/Gibco) +10% FBS (Atlas) to 70% confluence. Cells were plated in 6-well plates (Sarstedt) and grown to ∼60% confluency. Warm HBSS/Tyrodes 1:1 (2 mL) was replaced in each well, and the cells were treated with inhibitor dissolved in DMSO (0.2–50 μM, final concentration) for 30 min at 37 °C followed by the addition of [^{14}C]-arachidonic acid [8 μM, ∼2035 MBq/mmol, Perkin Elmer] for 30 min at 37 °C. Aliquots (400 μl) were removed and the reactions were terminated by solvent extraction in 400 μl ice-cold Et$_2$O/CH$_3$OH/1 M citrate, pH 4.0

(30:4:1). The organic phase was spotted on a 20 × 20 cm TLC plate (EMD Kieselgel 60, VWR). The plate was developed in EtOAc/ CH$_2$Cl$_2$/glacial AcOH (75:25:1), and radiolabeled prostaglandins were quantified with a radioactivity scanner (Bioscan, Inc., Washington, D.C.). The percentage of total products observed at different inhibitor concentrations was divided by the percentage of products observed for cells pre-incubated with DMSO.

4.2.3. Statistical analysis

The IC$_{50}$ values of the compounds reported in Table 3 and Fig. 3 and 4 were determined by nonlinear curve fitting using the GraphPad Prism program (GraphPad Prism Software (Windows version), Graph-Pad Software, Inc., San Diego, CA, USA) and are the mean ± SEM from three separate experiments.

4.3. Computational chemistry

Molecular modeling and graphics manipulations were performed using the molecular operating environment (MOE) [61] and UCSF-CHIMERA [62] software packages, running on a Linux workstation with an Intel Core i7 920 CPU and 12 GB of RAM. Figures were generated using Pymol 1.0 [63].

4.3.1. Ligand and receptor preparation

Model building and geometry optimizations of compounds **2f** and **2m** were accomplished with the MMFF94X force field, available within MOE. The crystal structures of ovine COX-1 in complex with celecoxib (PDB code: 3kk6) [37] and murine COX-2 complexed with SC-558 (PDB code: 6COX) [47] were used in the docking experiments. Bound ligands and water molecules were removed. A correct atom assignment for Asn, Gln, and His residues was done, and hydrogen atoms were added using standard MOE geometries. Partial atomic charges were computed by MOE using the Amber99 force field. All heavy atoms were then fixed, and hydrogen atoms were minimized using the AMBER99 force field and a constant dielectric of 1, terminating at a gradient of 0.001 kcal mol^{-1}• Å^{-1}.

4.3.2. Docking simulations

Docking of **2f** and **2m** to COX-1 and COX-2 was performed with GOLD version 5.0.1, which uses a genetic algorithm for determining the docking modes of ligands and proteins [38]. The coordinates of the cocrystallized ligand (celecoxib for COX-1 and SC-558 for COX-2) were chosen as an active-site origin. The active-site radius was set equal to 8 Å. The mobility of R120, S353, Y355 and S530 side chains was set up using the flexible sidechains option in the GOLD front end, which incorporates the Lovell rotamer library [64]. Each GA run used the default parameters of 100,000 genetic operations on an initial population of 100 members divided into five subpopulations, with weights for crossover, mutation, and migration being set to 95, 95, and 10, respectively. GOLD allows a user-definable number of GA runs per ligand, each of which starts from a different orientation. For these experiments, the number of GA runs was set to 200, and scoring of the docked poses was performed with the ChemPLP scoring function with ChemScore rescore. The best output poses (orientations) of the ligands generated were analyzed on the basis of ChemPLP/ChemScore score and H-bonding to the enzyme.

Acknowledgments

Appendix A. Supplementary data

Supplementary data associated with this article can be found in the online version, at http://dx.doi.org/10.1016/j.ejmech.2013.12.023. These data include MOL files and InChiKeys of the most important compounds described in this article.

References

[1] J.R. Vane, Inhibition of prostaglandin synthesis as a mechanism of action for aspirin-like drugs, Nature New Biol. 231 (1971) 232−235.

[2] D.L. Simmons, R.M. Botting, T. Hla, Cyclooxygenase isozymes: the biology of prostaglandin synthesis and inhibition, Pharmacol. Rev. 56 (2004) 387−437.

[3] T. Grosser, S. Fries, G.A. FitzGerald, Biological basis for the cardiovascular consequences of COX-2 inhibition: therapeutic challenges and opportunities, J. Clin. Invest. 116 (2006) 4−15.

[4] P. Patrignani, P. Filabozzi, C. Patrono, Selective cumulative inhibition of platelet thromboxane production by low-dose aspirin in healthy subjects, J. Clin. Invest. 69 (1982) 1366−1372.

[5] G.A. Fitzgerald, C. Patrono, The coxibs, selective inhibitors of cyclooxygenase-2, N. Engl. J. Med. 345 (2001) 433−442.

[6] M.S. Estevão, L.C.R. Carvalho, M. Freitas, A. Gomes, A. Viegas, J. Manso, S. Erhardt, E. Fernandes, E.J. Cabrita, M.M.B. Marques, Indole based cyclo-oxygenase inhibitors: synthesis, biological evaluation, docking and NMR screening, Eur. J. Med. Chem. 54 (2012) 823−833.

[7] M. Chen, E. Boilard, P.A. Nigrovic, P. Clark, D. Xu, G.A. Fitzgerald, L.P. Audoly, D.M. Lee, Predominance of cyclooxygenase 1 over cyclooxygenase 2 in the generation of proinflammatory prostaglandins in autoantibody-driven K/BxN serum-transfer arthritis, Arthritis Rheum. 58 (2008) 1354−1365.

[8] S. McClelland, S. Toomey, B. Hahren, D.J. Fitzgerald, O.A. Belton, Cyclo-oxygenase-1 gene deletion inhibits atherosclerosis in the ApoE$^{-/-}$ mouse model, Arterioscler. Thromb. Vasc. Biol. 24 (2004) e73, abst.

[9] P.C. Chulada, M.B. Thompson, J.F. Mahler, C.M. Doyle, B.W. Gaul, C. Lee, H.F. Tiano, S.G. Morham, O. Smithies, R. Langenbach, Genetic disruption of Ptgs-1, as well as Ptgs-2, reduces intestinal tumorigenesis in Min mice, Cancer Res. 60 (2000) 4705−4708.

[10] H.F. Tiano, C.D. Loftin, J. Akunda, C.A. Lee, J. Spalding, A. Sessoms, D.B. Dunson, E.G. Rogan, G. Morham, R.C. Smart, R. Langenbach, Deficiency of either cyclooxygenase (COX)-1 or COX-2 alters epidermal differentiation and reduces mouse skin tumorigenesis, Cancer Res. 62 (2002) 3395−3401.

[11] J.R. Barrio, N. Satyamurthy, S.C. Huang, A. Petric, G.W. Small, V. Kepe, Dissecting molecular mechanisms in the living brain of dementia patients, Acc. Chem. Res. 42 (2009) 842−850.

[12] M.G. Perrone, A. Scilimati, L. Simone, P. Vitale, Curr. Med. Chem. 17 (2010) 3769−3805.

[13] R.A. Gupta, L.V. Tejada, B.J. Tong, S.K. Das, J.D. Morrow, S.K. Dey, R.N. DuBois, Cyclooxygenase-1 is overexpressed and promotes angiogenic growth factor production in ovarian cancer, Cancer Res. 63 (2003) 906−911.

[14] X. Zhu, J.C. Eisenach, Cyclooxygenase-1 in the spinal cord is altered after peripheral nerve injury, Anesthesiology 99 (2003) 1175−1179.

[15] S.H. Choi, S. Aid, L. Caracciolo, S.S. Minami, T. Niikura, Y. Matsuoka, R.S. Turner, M.P. Mattson, F. Bosetti, Cyclooxygenase-1 inhibition reduces amyloid pathology and improves memory deficits in a mouse model of Alzheimer's disease, J. Neurochem. 124 (2013) 59−68.

[16] R. Calvello, M.A. Panaro, M.L. Carbone, A. Cianciulli, M.G. Perrone, P. Vitale, P. Malerba, A. Scilimati, Novel selective COX-1 inhibitors suppress neuro-inflammatory mediators in LPS-stimulated N13 microglial cells, Pharmacol. Res. 65 (2012) 137−148.

[17] V.H. Tran, C.C. Duke, E. Nurtjahja-Tjendraputra, A.J. Ammit, B.D. Roufogalis, Effective anti-platelet and COX-1 enzyme inhibitors from pungent constituents of ginger, Thromb. Res. 111 (2003) 259−265.

[18] T. Kitamura, T. Kawamori, N. Uchiya, M. Itoh, T. Noda, M. Matsuura, T. Sugimura, K. Wakabayashi, Inhibitory effects of mofezolac, a cyclooxygenase-1 selective inhibitor, on intestinal carcinogenesis, Carcinogenesis 23 (2002) 1463−1466.

[19] A. Tanaka, H. Sakai, Y. Motoyama, T. Ishikawa, H. Takasugi, Antiplatelet agents based on cyclooxygenase inhibition without ulcerogenesis. Evaluation and synthesis of 4,5-bis(4-methoxyphenyl)-2-substituted-thiazoles, J. Med. Chem. 37 (1994) 1189−1199.

[20] T. Ochi, Y. Motoyama, T. Goto, The analgesic effect profile of FR122047, a selective cyclooxygenase-1 inhibitor, in chemical nociceptive models, Eur. J. Pharmacol. 394 (2000) 49−54.

[21] M. Dohi, Y. Sakata, J. Seki, Y. Namikawa, J. Fujisaki, A. Tanaka, H. Takasugi, Y. Motoyama, K. Yoshida, The anti-platelet actions of FR122047, a novel cyclooxygenase inhibitor, Eur. J. Pharmacol. 243 (1993) 179−184.

[22] T. Ochi, T. Goto, Differential effect of FR122047, a selective cyclo-oxygenase-1 inhibitor, in rat chronic models of arthritis, Br. J. Pharmacol. 135 (2002) 782−788.

[23] X. Zheng, H. Oda, K. Takamatsu, Y. Sugimoto, A. Tai, E. Akaho, H.I. Ali, T. Oshiki, H. Kakuta, K. Sasaki, Analgesic agents without gastric damage: design and synthesis of structurally simple benzenesulfonanilide-type cyclooxygenase-1-selective inhibitors, Bioorg. Med. Chem. 15 (2007) 1014−1021.

[24] L. Di Nunno, P. Vitale, A. Scilimati, S. Tacconelli, P. Patrignani, Novel synthesis of 3,4-Diarylisoxazole analogues of valdecoxib: reversal COX-2 selectivity by sulfonamide group removal, J. Med. Chem. 47 (2004) 4881−4890.

[25] A. Scilimati, P. Vitale, L. Di Nunno, P. Patrignani, S. Tacconelli, M.L. Capone, Patent US 7 (2011) 989, 450 B2.

[26] P. Vitale, S. Tacconelli, M.G. Perrone, P. Malerba, L. Simone, A. Scilimati, A. Lavecchia, M. Dovizio, M. Marcantoni, A. Bruno, P. Patrignani, Synthesis, pharmacological characterization and docking analysis of a novel family of diarylisoxazoles as highly selective COX-1 inhibitors, J. Med. Chem. 56 (2013) 4277−4299.

[27] M.G. Perrone, P. Vitale, P. Malerba, A. Altomare, R. Rizzi, A. Lavecchia, C. Di Giovanni, E. Novellino, A. Scilimati, Diarylheterocycle core ring features effect in selective COX-1 inhibition, Chem. Med. Chem. 7 (2012) 629−641.

[28] M.G. Perrone, P. Malerba, Md. J. Uddin, P. Vitale, B.C. Crews, C.K. Daniel, K. Ghebreselasie, M.L. Nickels, M.N. Tantawy, H.C. Manning, L.J. Marnett, A. Scilimati, [18F]-P6 Analogue as PET Imaging Agent Targeting Cyclo-oxygenase-1, Eur. J. Med. Chem. (2014) submitted for publication.

[29] E.D. Thureson, K.M. Lakkides, C.J. Reke, Y. Sun, B.A. Wingerd, R. Micielli, A.M. Mulichak, M.G. Malkowski, R.M. Garavito, W.I. Smith, Prostaglandin endoperoxide H synthase-1. The functions of cyclooxygenase active site residues in the binding, positioning, and oxygenation of arachidonic acid, J. Biol. Chem. 276 (2001) 10347−10359.

[30] P. Vitale, A. Scilimati, Functional 3-Arylisoxazoles and 3-Aryl-2-isoxazolines from reaction of aryl nitrile oxides and enolates: synthesis and reactivity, Synthesis 45 (2013) 2940−2948.

[31] L. Di Nunno, A. Scilimati, P. Vitale, 5-Hydroxy-3-phenyl-5-vinyl-2-isoxazoline and 3-phenyl-5-vinylisoxazole: synthesis and reactivity, Tetrahedron 61 (2005) 11270−11278.

[32] L. Di Nunno, A. Scilimati, Synthesis of 3-aryl-4, 5-dihydro-5-hydroxy-1,2-oxazoles by reaction of substituted benzonitrile oxides with the enolate ion of acetaldehyde, Tetrahedron 43 (1987) 2181−2189.

[33] M.P. Bourbeau, J.T. Rider, A convenient synthesis of 4-alkyl-5-aminoisoxazoles, Org. Lett. 8 (2006) 3679−3680.

[34] P. Vitale, A. Scilimati, Five-membered ring heterocycles by reacting enolates with dipoles, Curr. Org. Chem. 17 (2013) 1986−2000.

[35] A. Scilimati, L. Di Nunno, P. Vitale, S. Tacconelli, P. Patrignani, S. Tacconelli, E. Porreca, L. Stuppia, Isoxazole derivatives and their use as cyclooxygenase inhibitors PCT Int. 2005, WO2005068442.

[36] P. Patrignani, M.R. Panara, A. Greco, O. Fusco, C. Natoli, S. Iacobelli, F. Cipollone, A. Ganci, C. Creminon, J. Maclouf, C. Patrono, Biochemical and pharmacological characterization of the cyclooxygenase activity of human blood prostaglandin endoperoxide synthases, J. Pharmacol. Exp. Ther. 271 (1994) 1705−1721.

[37] G. Rimon, R.S. Sidhu, D.A. Lauver, J.Y. Lee, N.P. Sharma, C. Yuan, R.A. Frieler, R.C. Trievel, B.R. Lucchesi, W.L. Smith, Coxibs interfere with the action of aspirin by binding tightly to one monomer of cyclooxygenase-1, Proc. Natl. Acad. Sci. U. S. A. 107 (2010) 28−33.

[38] G. Jones, P. Willett, R.C. Glen, A.R. Leach, R. Taylor, Development and validation of a genetic algorithm for flexible docking, J. Mol. Biol. 267 (1997) 727−748.

[39] M.L. Verdonk, J.C. Cole, M.J. Hartshorn, C.W. Murray, R.D. Taylor, Improved protein−ligand docking using GOLD, Proteins: Struct. Funct. Genet. 52 (2003) 609−623.

[40] O. Korb, T. Stutzlek, T.E. Exner, Empirical scoring functions for advanced protein-ligand docking with PLANTS, J. Chem. Inf. Model. 49 (2009) 84−96.

[41] J.W. Liebeschuetz, J.C. Cole, O. Korb, Pose prediction and virtual screening performance of GOLD scoring functions in a standardized test, J. Comput. Aided Mol. Des. 26 (2012) 737−748.

[42] G. Fracchiolla, A. Laghezza, L. Piemontese, P. Tortorella, F. Mazza, R. Montanari, G. Pochetti, A. Lavecchia, E. Novellino, S. Pierno, D. Conte Camerino, F. Loiodice, New 2-aryloxy-3-phenyl-propanoic acids as PPAR a/g dual agonists with improved potency and reduced adverse effects on skeletal muscle function, J. Med. Chem. 52 (2009) 6382−6393.

[43] C. La Motta, S. Sartini, L. Mugnaini, S. Salerno, F. Simorini, S. Taliani, A.M. Marini, F. Da Settimo, A. Lavecchia, E. Novellino, L. Antonioli, M. Fornai, C. Blandizzi, M. Del Tacca, Exploiting the pyrazolo[3,4-d]pyrimidin-4-one ring system as a useful template to obtain potent adenosine deaminase inhibitors, J. Med. Chem. 52 (2009) 1681−1692.

[44] L. Porcelli, F. Gilardi, A. Laghezza, L. Piemontese, N. Mitro, A. Azzariti, F. Altieri, L. Cervoni, G. Fracchiolla, M. Giudici, U. Guerrini, A. Lavecchia, R. Montanari, C. Di Giovanni, A. Paradiso, G. Pochetti, G.M. Simone, P. Tortorella, M. Crestani, F. Loiodice, Synthesis, characterization and biological evaluation of

ureidofibrate-like derivatives endowed with peroxisome proliferator activated receptor activity, J. Med. Chem. 55 (2012) 37–54.

[45] A. Laghezza, G. Pochetti, A. Lavecchia, G. Fracchiolla, S. Faliti, L. Piemontese, R. Montanari, C. Di Giovanni, V. Iacobazzi, V. Infantino, P. Tortorella, F. Loiodice, New 2-Aryloxy-3-phenyl-propanoic acids as potent peroxisome proliferator-activated receptors α/γ dual agonists able to upregulate the mitochondrial carnitine shuttle system gene expression, J. Med. Chem. 56 (2013) 60–72.

[46] N. Micale, R. Ettari, A. Lavecchia, C. Di Giovanni, K. Scarbaci, V. Troiano, S. Grasso, E. Novellino, T. Schirmeister, M. Zappalà, Development of peptidomimetic boronates as proteasome inhibitors, Eur. J. Med. Chem. 64 (2013) 23–34.

[47] R.G. Kurumbail, A.M. Stevens, J.K. Gierse, J.J. McDonald, R.A. Stegeman, J.Y. Pak, D. Gildehaus, J.M. Miyashiro, T.D. Penning, K. Seibert, P.C. Isakson, W.C. Stallings, Structural basis for selective inhibition of cyclooxygenase-2 by anti-inflammatory agents, Nature 384 (1996) 644–648.

[48] A.J. Vecchio, D.M. Simmons, M.G. Malkowski, J. Biol. Chem. 285 (2010) 22152–22163.

[49] E.D. Thuresson, M.G. Malkowski, K.M. Lakkides, C.J. Rieke, A.M. Mulichak, S.L. Ginell, R.M. Garavito, W.L. Smith, J. Biol. Chem. 276 (2001) 10358–10365.

[50] K. Gupta, B.S. Selinsky, C.J. Kaub, A.K. Katz, P.J. Loll, The 2.0 Å resolution crystal structure of prostaglandin H2 synthase-1: structural insights into an unusual peroxidase, J. Mol. Biol. 335 (2004) 503–518.

[51] C. Luong, A. Miller, J. Barnett, J. Chow, C. Ramesha, M.F. Browner, Flexibility of the NSAID binding site in the structure of human cyclooxygenase-2, Nat. Struct. Biol. 3 (1996) 927–933.

[52] D.K. Bhattacharyya, M. Lecomte, C.J. Rieke, M. Garavito, W.L. Smith, Involvement of arginine 120, glutamate 524, and tyrosine 355 in the binding of arachidonate and 2-phenylpropionic acid inhibitors to the cyclooxygenase active site of ovine prostaglandin endoperoxide H synthase-1, J. Biol. Chem. 271 (1996) 2179–2184.

[53] M.C. Walker, R.G. Kurumbail, J.R. Kiefer, K.T. Moreland, C.M. Koboldt, P.C. Isakson, K. Seibert, J.K. Gierse, A three-step kinetic mechanism for

[54] J. Suffert, Simple direct titration of organolithium reagents using N-pivaloyl-o-toluidine and/or N-pivaloyl-o-benzylaniline, J. Org. Chem. 54 (1989) 509–510.

[55] L. Di Nunno, A. Scilimati, P. Vitale, Regioselective synthesis and side-chain metallation and elaboration of 3-aryl-5-alkylisoxazoles, Tetrahedron 58 (2002) 2659–2665.

[56] L. Di Nunno, A. Scilimati, P. Vitale, Reaction of 3-phenylisoxazole with alkyl-lithiums, Tetrahedron 61 (2005) 2623–2630.

[57] A. Scilimati, P. Vitale, L. Di Nunno, P. Patrignani, S. Tacconelli, M.L. Capone, Functionalized diarylisoxazoles inhibitors of cyclooxygenase, Patent US 7 (2009) 989,450.

[58] L. Di Nunno, P. Vitale, A. Scilimati, L. Simone, F. Capitelli, Stereoselective dimerization of 3-arylisoxazoles to cage-shaped bis-β-lactams syn-2,6-diaryl-3,7-diazatricyclo[4.2.0.0^{2,5}]octan-4,8-diones induced by hindered lithium amides, Tetrahedron 63 (2007) 12388–12395.

[59] L. Di Nunno, P. Vitale, A. Scilimati, Effect of the aryl group substituent in the dimerization of 3-arylisoxazoles to syn 2,6-diaryl-3,7-diazatricyclo[4.2.0.0^{2,5}] octan-4,8-diones induced by LDA, Tetrahedron 64 (2008) 11198–11204.

[60] G.W. Gribble, C.F. Nutaitis, Reactions of sodium borohydride in acidic media. XVI. N-Methylation of amines with paraformaldehyde/trifluoroacetic acid, Synthesis 8 (1987) 709–711.

[61] Molecular Operating Environment (MOE), Version 2011.10, Chemical Computing Group, Inc., Montreal. Canada, 2011.

[62] E.F. Pettersen, T.D. Goddard, C.C. Huang, G.S. Couch, D.M. Greenblatt, E.C. Meng, T.E. Ferrin, UCSF chimera-A visualization system for exploratory research and analysis, J. Comput. Chem. 25 (2004) 1605–1612.

[63] W.L. DeLano, The PyMOL Molecular Graphics System, DeLano Scientific, San Carlos, CA, 2002.

[64] S.C. Lovell, J.M. Word, J.S. Richardson, D.C. Richardson, The penultimate rotamer library, Proteins 40 (2000) 389–408.